Electronic Supplementary Material (ESI) for RSC Advances.

Supplementary Information

Interfacial self-assembly of nanoporous C_{60} thin films

Jean-Nicolas Tisserant, Patrick A. Reissner, Sandra Jenatsch, Hannes Beyer, Roland Hany, Andreas Stemmer**

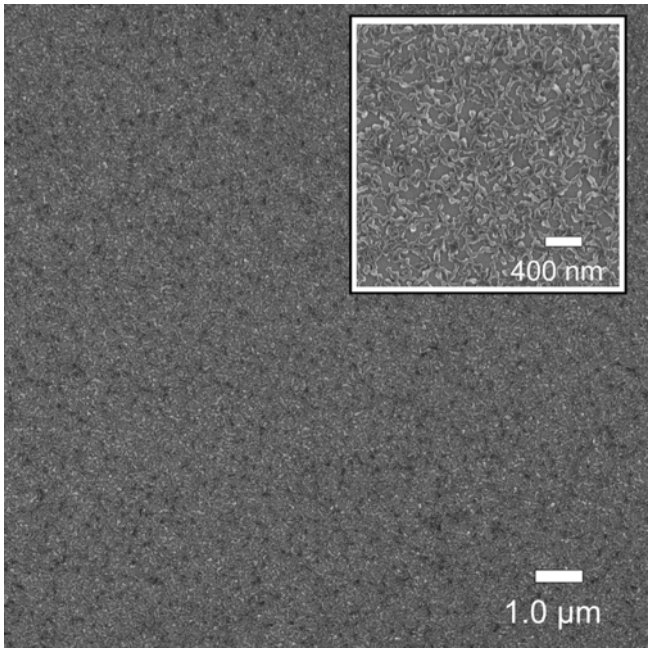

Figure S1. Large scale SEM image of a nanostructured C_{60} film and magnification (inset).

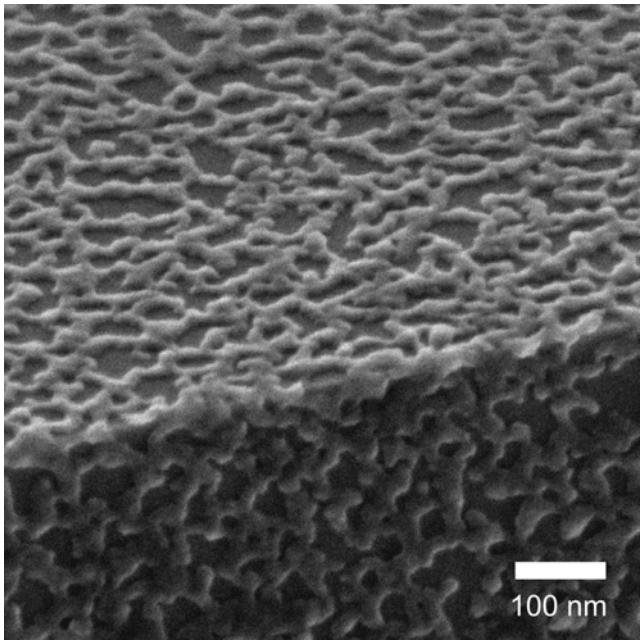

Figure S2. Flexibility of a C_{60} nanostructured thin film demonstrated by imaging over perpendicular surfaces of a silicon substrate.

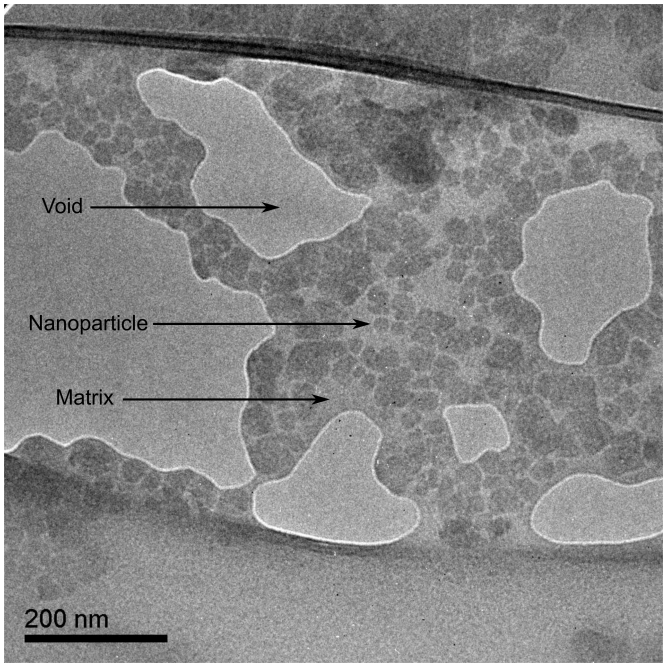

Figure S3. TEM image of a nanostructured C_{60} film. The image shows 10-50 nm large C_{60} particles embedded in a C_{60} matrix.

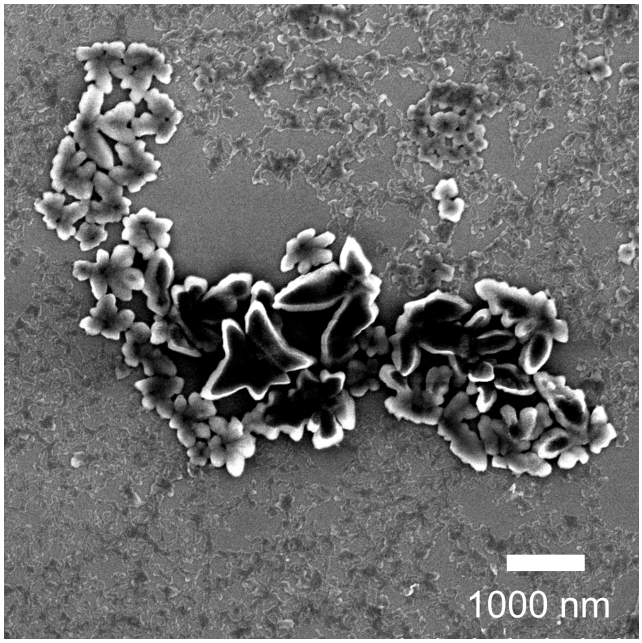

Figure S4. SEM image of a C_{60} film when depositing 250 µL $CHCl_3$ / C_{60} solution at P=500 mbar on an area of 3.5 cm^2. For volumes over ~200 μL, overgrowth of large C_{60} crystals occurs.

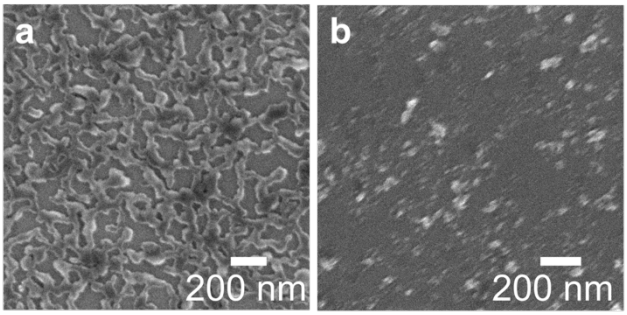

Figure S5. Solubility of C_{60} films deposited on Si without light-induced polymerization. SEM images (a) Pristine C_{60} film; (b) film residues after chloroform rinsing without prior light exposure.

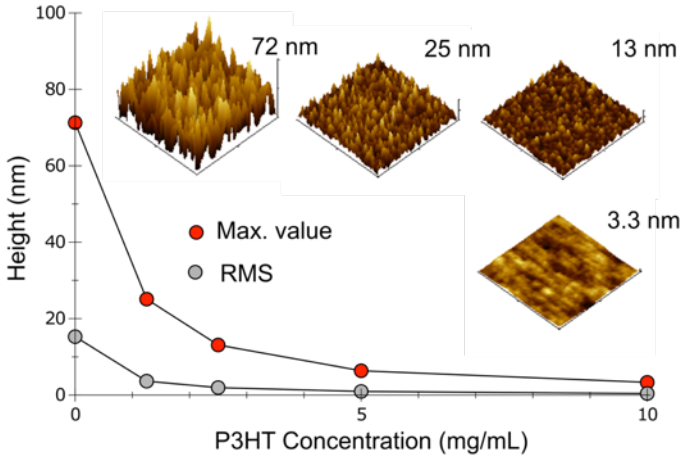

Figure S6. Infiltration of stabilized C_{60} nanostructures with P3HT. P3HT films were coated at 1000 rpm for 30 s from chloroform solutions. Red: maximum peak-to-valley

distance, grey: RMS roughness. Insets show SFM images of films obtained at 0, 1.25, 2.5 and 10 mg P3HT/mL.

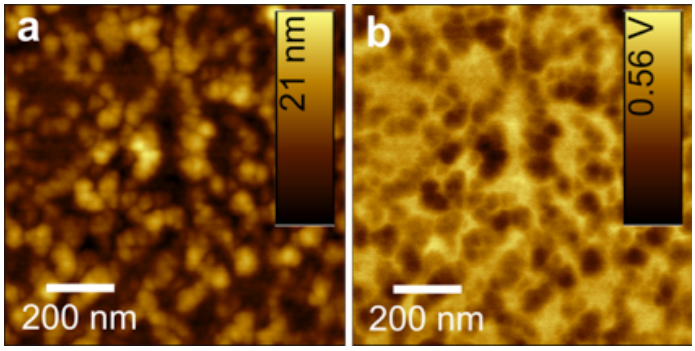

Figure S7. Scanning force microscopy images of nanostructured C_{60}, after light exposure and partial P3HT coating (2.5 mg/mL, 1000 rpm). (a) SFM topography showing reduced height difference and filling of the voids in the C_{60} layers, as well as the stability of the C_{60} domains; (b) Electrostatic force microscopy phase showing C_{60} domains (dark) and P3HT filling (bright).

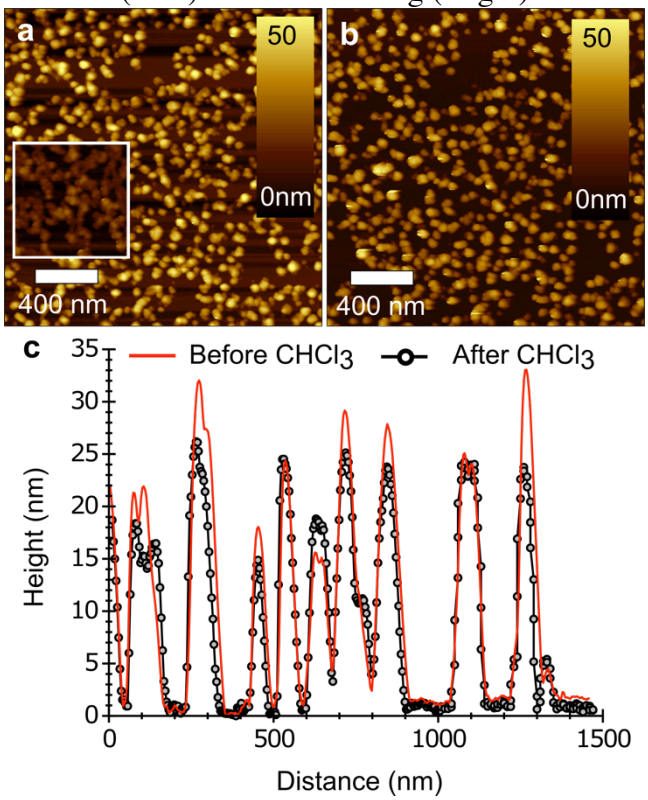

Figure S8. Evolution of the morphology upon film drying and consecutive film stabilization. (a) SFM image of a nano-structured C_{60} film after drying for 6 h at 80°C under nitrogen atmosphere and photo-polymerization, the inset shows the pristine film; (b) SFM image of the same area as (a) after solvent rinsing; (c) representative profiles extracted from (a) and (b).

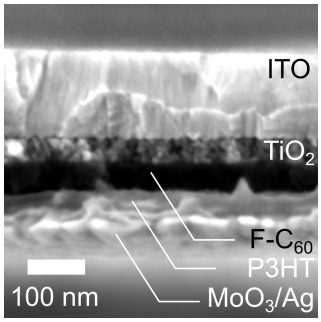

Figure S9. SEM cross-section image of a light-stabilized planar bilayer C_{60}/P3HT solar cell.

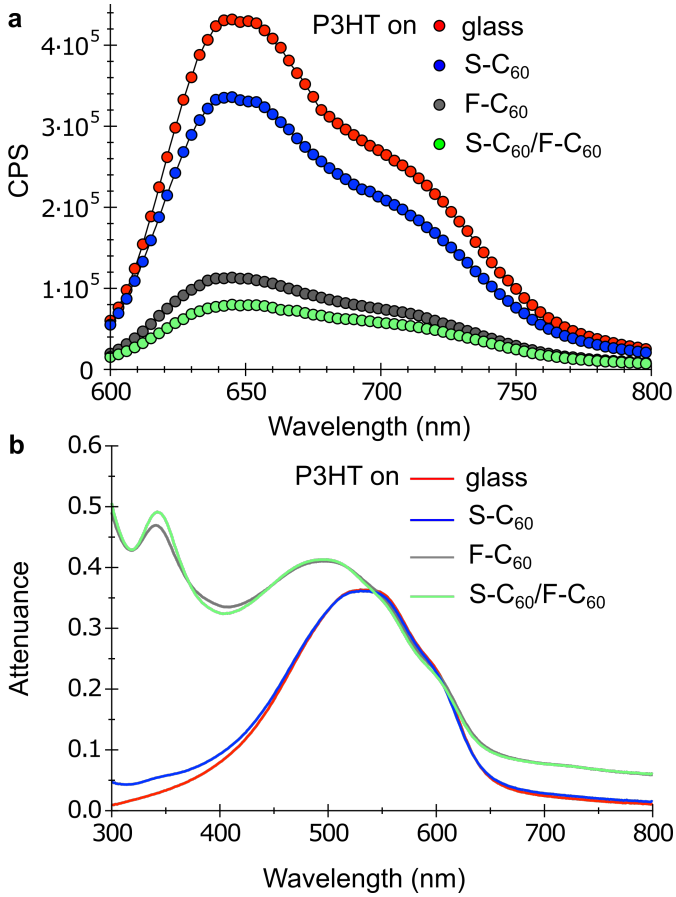

Figure S10. Photoluminescence of P3HT films, the excitation wavelength was at 550 nm, all C_{60} films were light-stabilized. (a) quenching of photoluminescence in architectures comparable to the ones used in solar cells, red: pristine P3HT, blue: on S-C_{60}, grey: on F-C_{60}, green; on F-C_{60} + S-C_{60}. The photoluminescence intensity drops by 30% at 643 nm between F-C_{60} and S-C_{60}/F-C_{60}. (b) UV-Vis of corresponding films showing a constant P3HT absorption.

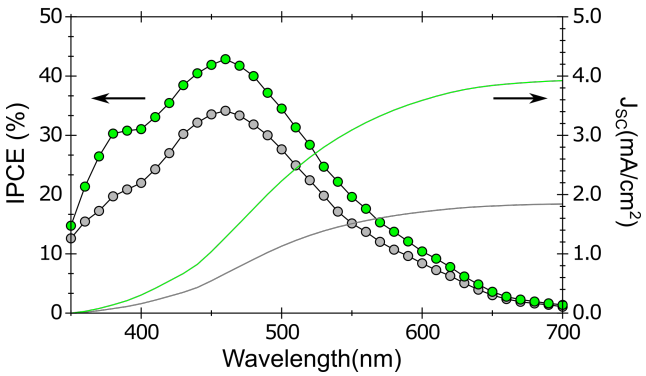

Figure S11. Internal photon-to-current conversion efficiency (IPCE) measurements and corresponding J_{SC}. grey: F-C_{60}, green: 2 layers S-C_{60} on F-C_{60}.